Magnetic and noncentrosymmetric Weyl fermion semimetals in the RAlGe family of compounds (R=rareearth)

Chang, Guoqing ; Singh, Bahadur ; Xu, Su-Yang ; Bian, Guang ; Huang, Shin-Ming ; Hsu, Chuang-Han ; Belopolski, Ilya ; Alidoust, Nasser ; Sanchez, Daniel S ; Zheng, Hao ; Lu, Hong ; Zhang, Xiao ; Bian, Yi ; Chang, Tay-Rong ; Jeng, Horng-Tay ; Bansil, Arun ; Hsu, Han ; Jia, Shuang ; Neupert, Titus ; Lin, Hsin ; Hasan, M Zahid

Abstract: Weyl semimetals are novel topological conductors that host Weyl fermions as emergent quasiparticles. In this Rapid Communication, we propose a new type of Weyl semimetal state that breaks both time-reversal symmetry and inversion symmetry in the RAlGe (R=rare−earth) family. Compared to previous predictions of magnetic Weyl semimetal candidates, the prediction of Weyl nodes in RAlGe is more robust and less dependent on the details of the magnetism because the Weyl nodes are generated already by the inversion breaking and the ferromagnetism acts as a simple Zeeman coupling that shifts the Weyl nodes in k space. Moreover, RAlGe offers remarkable tunability, which covers all varieties of Weyl semimetals including type I, type II, inversion breaking, and time-reversal breaking, depending on a suitable choice of the rare-earth elements. Furthermore, the unique noncentrosymmetric and ferromagnetic Weyl semimetal state in RAlGe enables the generation of spin currents.

DOI: https://doi.org/10.1103/physrevb.97.041104

Rapid Communications

Magnetic and noncentrosymmetric Weyl fermion semimetals in the *R*AlGe family of compounds (*R* = rare earth)

Guoqing Chang,[1,2] Bahadur Singh,[1,2] Su-Yang Xu,[3,*] Guang Bian,[3,4] Shin-Ming Huang,[5] Chuang-Han Hsu,[1,2] Ilya Belopolski,[3] Nasser Alidoust,[3] Daniel S. Sanchez,[3] Hao Zheng,[3,6] Hong Lu,[7] Xiao Zhang,[7] Yi Bian,[7] Tay-Rong Chang,[8,9] Horng-Tay Jeng,[8,10] Arun Bansil,[11] Han Hsu,[12] Shuang Jia,[7,13] Titus Neupert,[14,15] Hsin Lin,[1,2,†] and M. Zahid Hasan[3,16,‡]

[1]*Centre for Advanced 2D Materials and Graphene Research Centre National University of Singapore, 6 Science Drive 2, Singapore 117546*

[2]*Department of Physics, National University of Singapore, 2 Science Drive 3, Singapore 117542*

[3]*Department of Physics, Laboratory for Topological Quantum Matter and Spectroscopy (B7), Princeton University, Princeton, New Jersey 08544, USA*

[4]*Department of Physics and Astronomy, University of Missouri, Columbia, Missouri 65211, USA*

[5]*Department of Physics, National Sun Yat-sen University, Kaohsiung 804, Taiwan*

[6]*School of Physics and Astronomy, Shanghai Jiao Tong Univeristy, 200240 Shanghai, China*

[7]*International Center for Quantum Materials, School of Physics, Peking University, China*

[8]*Department of Physics, National Tsing Hua University, Hsinchu 30013, Taiwan*

[9]*Department of Physics, National Cheng Kung University, Tainan 701, Taiwan*

[10]*Institute of Physics, Academia Sinica, Taipei 11529, Taiwan*

[11]*Department of Physics, Northeastern University, Boston, Massachusetts 02115, USA*

[12]*Department of Physics, National Central University, Jhongli City, Taoyuan 32001, Taiwan*

[13]*Collaborative Innovation Center of Quantum Matter, Beijing 100871, China*

[14]*Princeton Center for Theoretical Science, Princeton University, Princeton, New Jersey 08544, USA*

[15]*Department of Physics, University of Zurich, Winterthurerstrasse 190, 8057 Zurich, Switzerland*

[16]*Princeton Institute for Science and Technology of Materials, Princeton University, Princeton, New Jersey 08544, USA*

(Received 16 December 2016; revised manuscript received 28 February 2017; published 9 January 2018)

Weyl semimetals are novel topological conductors that host Weyl fermions as emergent quasiparticles. In this Rapid Communication, we propose a new type of Weyl semimetal state that breaks both time-reversal symmetry and inversion symmetry in the *R*AlGe (*R* = rare-earth) family. Compared to previous predictions of magnetic Weyl semimetal candidates, the prediction of Weyl nodes in *R*AlGe is more robust and less dependent on the details of the magnetism because the Weyl nodes are generated already by the inversion breaking and the ferromagnetism acts as a simple Zeeman coupling that shifts the Weyl nodes in *k* space. Moreover, *R*AlGe offers remarkable tunability, which covers all varieties of Weyl semimetals including type I, type II, inversion breaking, and time-reversal breaking, depending on a suitable choice of the rare-earth elements. Furthermore, the unique noncentrosymmetric and ferromagnetic Weyl semimetal state in *R*AlGe enables the generation of spin currents.

DOI: 10.1103/PhysRevB.97.041104

Finding new quantum materials with useful properties is one of the frontiers of modern condensed-matter physics and material science [1–6]. The recent realization of a nonmagnetic Weyl semimetal state in the TaAs class of materials [7–25] has attracted significant attention. Further transport measurements have revealed unconventional magnetic and optical responses of the TaAs family [26–29]. Despite recent advances of topological semimetals in both theory [30–43] and experiment [26–29,44–51], the ferromagnetic Weyl semimetal [8,9,52–57] has not been realized in experiments. A key issue is that first-principles band-structure calculations on these magnetic materials (e.g., iridates [8] and $HgCr_2Se_4$ [52]) are quite challenging. For example, the all-in (all-out) magnetic structures in iridates appeared to be complicated to verify in experiments [53] and model in first-principles calculations [8,54]. Also, for many magnetic materials, such as $HgCr_2Se_4$, the magnetic band structure may be very sensitive to the details of the magnetism. As a result, the first-principles prediction of Weyl nodes in magnetic compounds is not as robust as that in nonmagnetic compounds, such as TaAs [10,11]. Here, we propose a different strategy to search for magnetic Weyl semimetals. Taking advantage of the Weyl nodes generated by inversion symmetry breaking in the nonmagnetic compound LaAlGe [44,58], we present a new type of magnetic Weyl semimetal in its isostructural sister compounds CeAlGe and PrAlGe [59,60] that are ferromagnetic [61–63]. We show that the ferromagnetism in *R*AlGe can be modeled more reliably in first-principles calculations as it is found to not completely change the band structure. Rather, it acts as a Zeeman coupling and splits the spin-up and spin-down bands, which shifts the Weyl nodes in *k* space to break time-reversal symmetry. For these reasons, the prediction of Weyl nodes in *R*AlGe is less dependent on the details of the magnetism. Moreover, we show

*Corresponding author: suyangxu@princeton.edu
†Corresponding author: nilnish@gmail.com
‡Corresponding author: mzhasan@princeton.edu

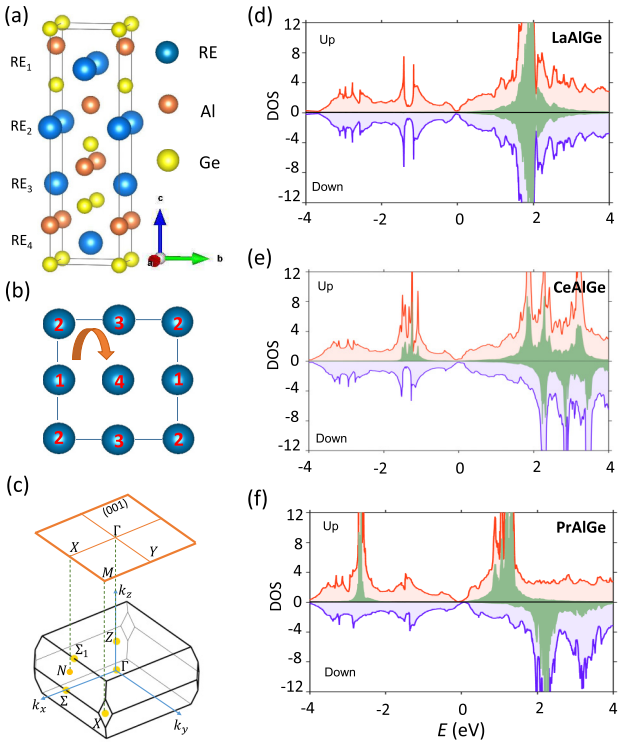

FIG. 1. Lattice structure, Brillouin zone (BZ), and density of state (DOS) of RAlGe (R = La, Ce, and Pr). (a) Body-centered tetragonal structure of RAlGe with space-group $I4_1md$ (109). The structure consists of stacks of rare-earth elements (RE), Al, and Ge layers, and along the (001) direction each layer consists of only one type of element. (b) The schematic of the RE atomic layer showing the skew axis along the c axis. (c) The bulk and (001) surface BZ. (d)–(f) First-principles DOS of (d) LaAlGe, (e) CeAlGe, and (f) PrAlGe. The partial DOS for spin-up and spin-down states are plotted in red and violet colors, respectively. The DOS from localized f orbitals are drawn in green color.

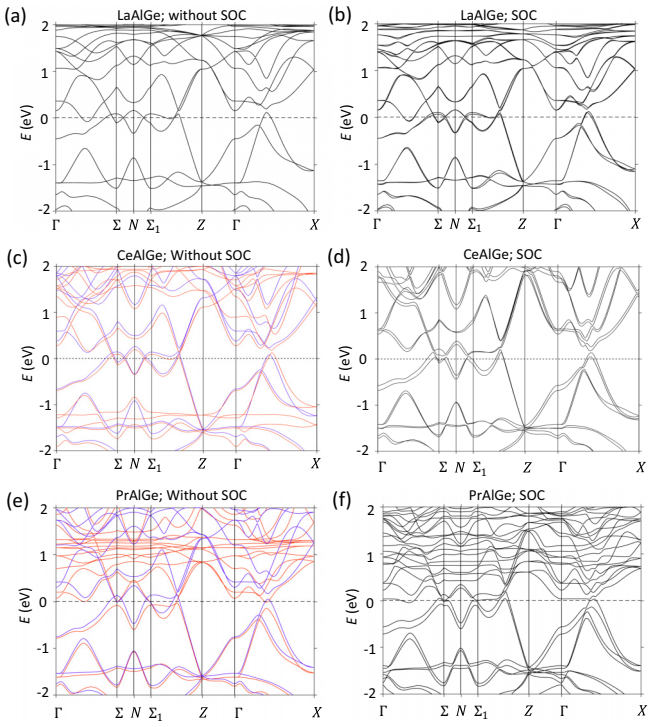

FIG. 2. First-principles band structure of RAlGe (R = La, Ce, and Pr). (a) and (b) Calculated bulk band structure of LaAlGe without and with the inclusion of spin-orbit coupling. (c) and (d) Bulk band structure of CeAlGe without and with the inclusion of spin-orbit coupling. In (c) the bands of spin-up and spin-down states are plotted in red and violet colors, respectively. (e) and (f) The same as in (c) and (d) but for PrAlGe.

that the RAlGe family offers remarkable tunability where type-I, type-II [30], inversion-breaking, and time-reversal-breaking types of Weyl semimetal states are all available. Furthermore, as recently predicted in theory [64], the time-reversal and inversion-breaking Weyl semimetals uniquely can induce a quantum spin current without a concomitant charge current. In addition, whereas a noncentrosymmetric (magnetic) Weyl semimetal is an intermediate phase between a trivial insulator and a three-dimensional (3D) topological insulator (a 3D stacked Chern insulator) state [65], here, with both symmetries broken, the phase diagram may be even richer. This rich phase diagram potentially may be explored via doping or chemical substitution.

RAlGe crystallizes in a body-centered tetragonal Bravais lattice with an $\mathcal{I}$-breaking space-group $I4_1md$ (109) [58–60] [Figs. 1(a) and 1(b)]. Our results show that LaAlGe is nonmagnetic, whereas CeAlGe and PrAlGe are ferromagnetic with their magnetization easy axes along the a and c directions, respectively. For CeAlGe, the calculated magnetic moment is $1\mu_B$ per Ce atom, and the experimental measured value is $0.94\mu_B$ [61]. For PrAlGe, the calculated magnetic moment is $2\mu_B$ per Pr atom, whereas the experimental value has not been reported in literature. Figures 1(d)–1(f) show the calculated DOS without spin-orbit coupling (SOC) for RAlGe. The DOS of the majority and minority spin states are colored in red and blue. It can be seen clearly that in LaAlGe the DOS of the two spins are equal, consistent with its nonmagnetic nature. In contrast, an imbalance between the DOS of the majority and minority spin states is seen in CeAlGe and PrAlGe, suggesting a ferromagnetic ground state in agreement with the experimental findings [62,63]. The green shaded areas are the DOS of the f electrons. The electronic configuration of the La atom is [Xe]$6s^2 5d^1 4f^0$, meaning that all f orbitals are empty. Indeed, Fig. 1(d) shows that all the f electrons are in the conduction bands. On the other hand, a Ce (or Pr) atom should have one (or two) electrons occupying the f orbitals. As a result, we see some f bands below the Fermi level in Figs. 1(e) and 1(f). Moreover, our calculations [Figs. 1(e) and 1(f)] show that the occupied f-electron states in CeAlGe and PrAlGe clearly are spin polarized. These results suggest that the ferromagnetic coupling between the f-electrons' local moments lead to ferromagnetism in CeAlGe and PrAlGe, which, in turn, makes the conduction electrons (s, p, d orbitals) near the Fermi level also spin polarized. Furthermore, our band-structure calculations without SOC [Figs. 2(c) and 2(e)] clearly show a spin splitting in the electronic states. These results confirm our conceptual picture: The ferromagnetism arises from the ordering of the f-electrons' local moments.

These local moments serve as an effective Zeeman field and make the conduction (s,p,d orbital) bands spin polarized. We highlight the fact that the ferromagnetism can be treated as a Zeeman coupling and does not completely change the band structure at low energies. In the presence of SOC, the spin-up and spin-down states are further mixed by Rashba/Dresselhaus interactions due to the lack of inversion symmetry, making spin not a good quantum number. Thus, we do not color code the bands in Figs. 2(d) and 2(f).

In order to explain the Weyl nodes in CeAlGe and PrAlGe, we start from the nonmagnetic compound LaAlGe. In the absence of spin-orbit coupling, the crossing between conduction and valence bands yields four nodal lines on the $k_x = 0$ and $k_y = 0$ mirror planes and four pairs of (spinless) Weyl nodes on the $k_z = 0$ plane, which we denoted as $W3$ [44]. Upon the inclusion of the spin-orbit coupling, the nodal lines are gapped out, and 24 Weyl nodes emerge in the vicinity. We refer to the 8 Weyl nodes located on the $k_z = 0$ plane as $W1$ and the remaining 16 Weyl nodes away from this plane as $W2$ [44]. Moreover, each $W3$ (spinless) Weyl node splits into two (spinful) Weyl nodes of the same chirality, which we call $W3'$ and $W3''$ [44]. Hence, in total there are 40 Weyl nodes for LaAlGe [44].

We now turn to the Weyl semimetal states in CeAlGe and PrAlGe. We conceptually consider a temperature-dependent evolution. Starting at a higher temperature above the Curie transition, we expect the Ce(Pr)AlGe sample to already become a Weyl semimetal because of the broken space-inversion symmetry with 40 Weyl nodes as in LaAlGe. Now we lower the temperature below the Curie temperature, the effect of the ferromagnetism in CeAlGe and PrAlGe can be understood qualitatively as a Zeeman coupling to the conduction electron states. To the lowest order, we expect that this will shift the Weyl nodes in a way that their momentum space configuration reflects the time-reversal symmetry breaking. We use this picture to understand the calculated results of the Weyl nodes' configuration of these two compounds. In CeAlGe, indeed, we found that the Weyl nodes are still the $W1$, $W2$, and $W3$ as in LaAlGe [Figs. 3(a) and 3(b)]. The difference is that they are shifted away from the original location due to magnetism. In LaAlGe all $W1$ nodes can be related by symmetry operations. However, in CeAlGe, the inclusion of a magnetization along the a direction gives rise to four inequivalent $W1$ Weyl nodes. They have different momentum space locations and energies. Similarly, there are now four inequivalent $W2$ and eight inequivalent $W3$ Weyl nodes in CeAlGe because of the reduction of symmetries by the inclusion of the magnetization. In PrAlGe, the magnetization along the c axis leads to one inequivalent $W1$, two inequivalent $W2$, and two inequivalent $W3$ Weyl nodes. In addition, we find that the inclusion of ferromagnetization in PrAlGe may introduce new Weyl nodes, which we denote as the $W4$ nodes [Figs. 3(c)–3(e)]. The chiral charges of the Weyl points in RAlGe are determined by the net Berry flux passing through the two-dimensional (2D) manifold that encloses the Weyl fermions [8].

In order to understand how the Weyl nodes are shifted by the magnetization, we discuss the symmetry constraints in the presence of the ferromagnetic order in CeAlGe and PrAlGe.

In CeAlGe, the magnetization is oriented along the a axis. Both $\mathcal{T}$ and C_2 reverse this in-plane magnetization. However, their product $C_2\mathcal{T}$ is still a symmetry of the magnetic system, and the same is true for M_x. Thus, all symmetry-nonequivalent Weyl nodes are found in the $k_x > 0$ part of the BZ depicted in Fig. 3(b). Due to $C_2\mathcal{T}$, all $W1$- and $W3$-derived Weyl nodes are still pinned to $k_z = 0$, and the $W2$-derived nodes are found in $\pm k_z$ pairs. It is also interesting to note that the movement of all the Weyl nodes in the vicinity of the $M_y(\|k_x)$ mirror plane (W_1^1, W_1^2, W_2^2, and W_2^3) is much more significant than those of the $M_x(\|k_y)$ mirror plane (W_1^3, W_1^4, W_2^1, and W_2^4). This phenomenon is also symmetry related. Specifically, the Weyl nodes near the $M_x(\|k_y)$ mirror plane are roughly stationary upon magnetization because the symmetries $C_2\mathcal{T}$ and M_x are the only constraints to the effective Hamiltonian near the M_x mirror plane [10,11]. However, this term turns out to be only relevant for the energy but not for the position of the Weyl nodes. The detailed information of the Weyl nodes including the momentum space locations, the energies, and the type, is shown in the Supplemental Material, Sec. C [66].

In PrAlGe, the magnetization is oriented along z. Both $\mathcal{T}$ and any of the mirror and glide mirror symmetries reverse this magnetization. However, their products, e.g., $\mathcal{T}M_x$, are still a symmetry of the magnetic system. Furthermore, C_{2z} and $\bar{C}_{4z}$ are preserved by the magnetization. Thus, all symmetry-nonequivalent Weyl nodes are found in a quadrant of the BZ depicted in Fig. 3(d). The main difference to LaAlGe is that $C_{2z}\mathcal{T}$ symmetry is broken. As a result, we expect the $W1$ and $W3$ Weyl nodes to move along the k_z direction and become no longer pinned to $k_z = 0$. On the other hand, the $W2$ Weyl nodes are expected to stop appearing in $\pm k_z$ pairs.

Our theoretical discovery of CeAlGe and PrAlGe reveals a new route for realizing $\mathcal{T}$-breaking Weyl fermions. The traditional and commonly accepted proposal for realizing $\mathcal{T}$-breaking Weyl fermions is to break the time-reversal symmetry of a 3D Dirac fermion system as shown in Figs. 4(a) and 4(b). In this way, the Weyl fermions actually arise from the breaking of the time-reversal symmetry. We can qualitatively understand the anomalous Hall effect. As shown in Fig. 4(b), we consider the Chern number of a series of (k_y,k_z) 2D slices at different k_x intercepts. Any slice between the left boundary of the BZ and the first dotted line has a Chern number of 0. As we continue sweeping the (k_y,k_z) slice to the right, we pass through the blue Weyl node, and therefore the Chern number changes by 1. Consequently, a slice between the first dotted line and the second dotted line has a Chern number of 1. Then we pass the red Weyl node, and the Chern number of a slice between the second dotted line and the right boundary of the BZ is 0. As a result, the Chern number averaged over all k_z's in the BZ is nonzero, which demonstrates the existence of an anomalous Hall effect. It can be checked that this simple consideration carries over to CeAlGe and PrAlGe despite the presence of additional symmetries, and an anomalous Hall effect is expected on the plane perpendicular to the respective magnetization. By contrast, in the Dirac semimetal case in Fig. 4(a), the Chern number of any slice is zero, consistent with the fact that Dirac semimetals do not show anomalous Hall conductance. In terms of experimental realization, this proposal means that one needs to introduce magnetism to a Dirac semimetal system, such as $TlBi(S_{1-x}Se_x)_2$, Cd_3As_2, and

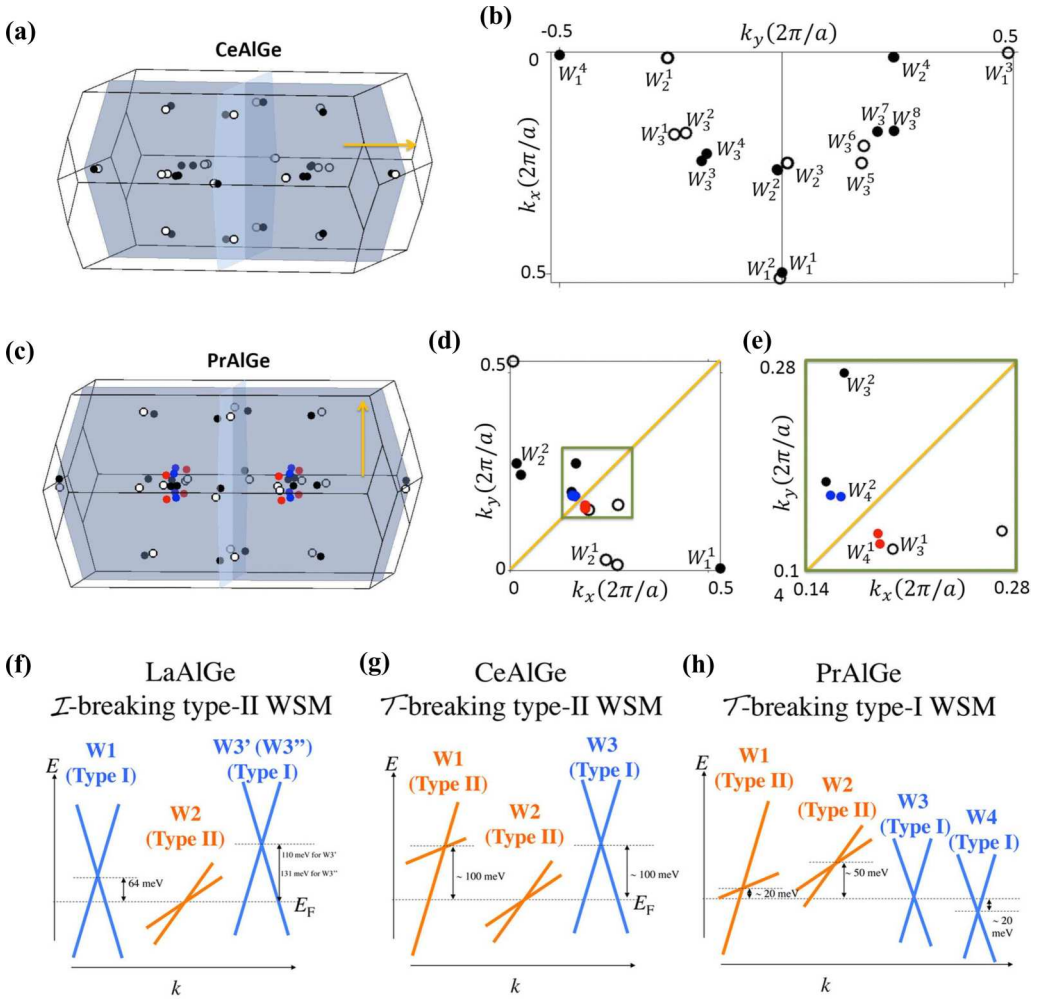

FIG. 3. Weyl fermions in LaAlGe, CeAlGe, and PrAlGe. (a) and (c) Weyl nodes (denoted by $W3$) in the first BZ of CeAlGe and PrAlGe with SOC. The arrows indicate the magnetization orientation. The red and blue dots denote the new Weyl nodes ($W4$) generated by the magnetization of the f orbitals of Pr. (b) Projection of the Weyl nodes on the (001) surface Brillouin zone (SBZ) of CeAlGe. The configuration of the other half of the SBZ can be obtained by considering mirror symmetry. (d) and (e) The same as in (b) but for PrAlGe. (f)–(h) Schematics of the band dispersion of the Weyl fermions in LaAlGe, CeAlGe, and PrAlGe, respectively.

Na_3Bi. Since these materials are nonmagnetic, one will need to dope the system with magnetic dopants, which has been proven to be quite difficult. It is also challenging to systematically study the band structure of the magnetically doped system through first-principles calculations.

We now elaborate on our new route for realizing $\mathcal{T}$-breaking Weyl fermions as demonstrated in CeAlGe and PrAlGe. Rather than starting from a Dirac semimetal, we start from a space-inversion- ($\mathcal{I}$-) breaking Weyl semimetal. As schematically shown in Fig. 4(c), two pairs of Weyl nodes are generated by the breaking of space inversion symmetry. In this case, magnetization is only responsible for shifting the momentum space location of the Weyl nodes. We note that a $\mathcal{T}$-breaking Weyl semimetal is defined as the breaking of the time-reversal symmetry in terms of the Weyl node configuration. Specifically, Weyl nodes of the same chirality cannot appear at opposite momenta ($\pm\vec{k}$). Therefore, although in this case the Weyl fermions do not arise from ferromagnetism, the system in Fig. 4(d) still counts as a $\mathcal{T}$-breaking Weyl semimetal. This can also be seen by studying the Chern number of the (k_y,k_z) 2D slices. As shown in Figs. 4(c) and 4(d), introducing magnetism leads to a finite k_x range at which the Chern number of the (k_y,k_z) 2D slice is nonzero. This also suggests the existence of anomalous Hall conductance in the system shown in Fig. 4(d). We emphasize a number of advantages of this new route. Introducing magnetism is performed by going from LaAlGe to CeAlGe or PrAlGe rather than doping. This not only avoids the complicated doping processes, but also enables systematically understanding the band structure in calculations as we have achieved here. Furthermore, our results demonstrate an entirely different way to search for $\mathcal{T}$-breaking Weyl semimetals in the future, i.e., to look for the isochemical ferromagnetic cousin compounds of an $\mathcal{I}$-breaking Weyl semimetal.

Finally, we highlight the tunability of the RAlGe family. As we have shown here, the low-energy band structures of LaAlGe, CeAlGe, and PrAlGe realize the $\mathcal{I}$-breaking type-II, the $\mathcal{T}$-breaking type-II, and the $\mathcal{T}$-breaking type-I Weyl fermions. Moreover, n (electron) doping can be achieved by changing the ratio between Al and Ge, i.e., $RAl_{1-x}Ge_{1+x}$ [60]. In the weak-disorder limit ($x \ll 1$), which cannot localize

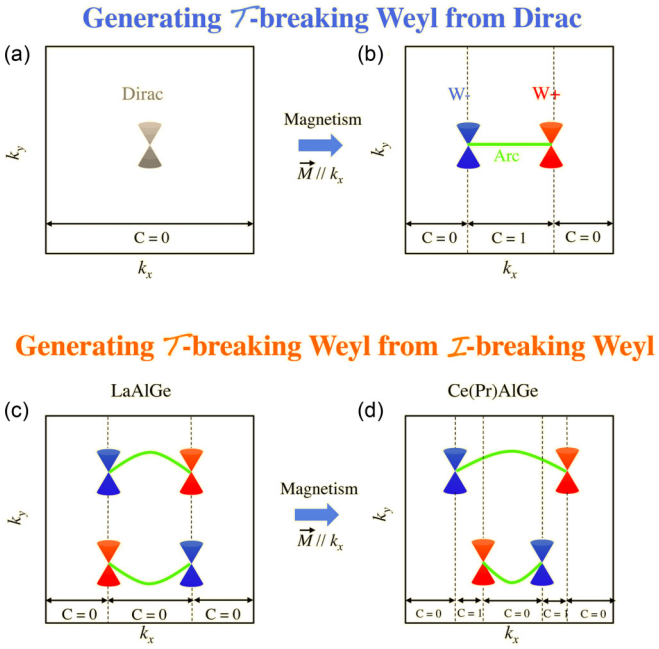

FIG. 4. A new route for generating magnetic Weyl fermions. (a) and (b) The Dirac node in a Dirac semimetal splits into a pair of Weyl nodes upon the inclusion of a magnetic field. The Weyl nodes are connected by a Fermi arc surface state. (c) and (d) Two pairs of Weyl nodes are present in an inversion-breaking Weyl semimetal. The Weyl nodes are shifted in momentum space upon the inclusion of a magnetic field, generating regions in **k** space with a nonzero Chern number.

the conduction electrons from the Weyl fermions [67,68], the doping will enable one to access other Weyl nodes that are above the Fermi level [Figs. 3(f)–3(h)]. In general, *R*AlGe is an extremely rich system that enables one to systematically study all types of Weyl fermions in a single family.

Work at Princeton University was supported by the US Department of Energy under Basic Energy Sciences (Grant No. DOE/BES DE-FG-02-05ER46200). M.Z.H. acknowledges Visiting Scientist support from Lawrence Berkeley National Laboratory and partial support from the Gordon and Betty Moore Foundation for theoretical work. The work at the National University of Singapore was supported by the National Research Foundation, Prime Minister's Office, Singapore under its NRF fellowship (NRF Award No. NRF-NRFF2013-03). S.J. acknowledges support by the National Science Foundation of China Grant No. 11774007 and the National Basic Research Program of China Grant No. 2014CB239302. The work at Northeastern University was supported by the US Department of Energy (DOE), Office of Science, Basic Energy Sciences Grant No. DE-FG02-07ER46352 and benefited from Northeastern University's Advanced Scientific Computation Center (ASCC) and the NERSC supercomputing center through DOE Grant No. DE-AC02-05CH11231. T.N. acknowledges support by the Swiss National Science Foundation (Grant No. 200021-169061) and the ERC-StG-Neupert-757867-PARATOP, respectively. The work at the National Sun Yat-sen University was supported by the Ministry of Science and Technology in Taiwan under Grant No. MOST105-2112-M110-014-MY3. T.-R.C. and H.-T.J. were supported by the Ministry of Science and Technology. T.-R.C. was supported by the National Cheng Kung University. T.-R.C. and H.-T.J. also thank the National Center for Theoretical Sciences (NCTS) for technical support. H.H. was supported by the Ministry of Science and Technology of Taiwan under Grant No. MOST 104-2112-M-008-005-MY3.

G.C., B.S., and S.-Y.X. contributed equally to this work.

[1] M. Z. Hasan and C. L. Kane, Rev. Mod. Phys. **82**, 3045 (2010).
[2] X.-L. Qi and S.-C. Zhang, Rev. Mod. Phys. **83**, 1057 (2011).
[3] M. Z. Hasan, S.-Y. Xu, and M. Neupane, in *Topological Insulators: Fundamentals and Perspectives*, edited by F. Ortmann, S. Roche, and S. O. Valenzuela (Wiley, Hoboken, NJ, 2015).
[4] M. Z. Hasan, S.-Y. Xu, and G. Bian, Phys. Scr. T **T164**, 014001 (2015).
[5] M. Z. Hasan, S.-Y. Xu, I. Belopolski, and S.-M. Huang, Annu. Rev. Condens. Matter Phys. **8**, 289 (2017).
[6] A. Bansil, H. Lin, and T. Das, Rev. Mod. Phys. **88**, 021004 (2016).
[7] H. Weyl, Z. Phys. **56**, 330 (1929).
[8] X. Wan, A. M. Turner, A. Vishwanath, and S. Y. Savrasov, Phys. Rev. B **83**, 205101 (2011).
[9] A. A. Burkov and L. Balents, Phys. Rev. Lett. **107**, 127205 (2011).
[10] S.-M. Huang, S.-Y. Xu, I. Belopolski, C-C. Lee, G. Chang, B. Wang, N. Alidoust, G. Bian, M. Neupane, C. Zhang, S. Jia, A. Bansil, H. Lin, and M. Z. Hasan, Nat. Commun. **6**, 7373 (2015).
[11] H. Weng, C. Fang, Z. Fang, A. Bernevig, and X. Dai, Phys. Rev. X **5**, 011029 (2015).
[12] S.-Y. Xu, I. Belopolski, N. Alidoust, M. Neupane, G. Bian, C. Zhang, R. Sabkar, G. Chang, Z. Yuan, C-C. Lee, S.-M. Huang, H. Zheng, J. Ma, D. S. Sanchez, B. Wangm, A. Bansil, F. Chou, P. P. Shibayev, H. Lin, S. Jia, and M. Z. Hasan, Science **349**, 613 (2015).
[13] L. Lu, Z. Wang, D. Ye, L. Ran, L. Fu, J. D. Joannopoulos, and M. Soljačić, Science **349**, 622 (2015).
[14] B. Q. Lv, H. Weng, B. B. Fu, X. P. Wang, H. Miao, J. Ma, P. Richard, X. C. Huang, L. X. Zhao, G. F. Chen, Z. Fang, X. Dai, T. Qian, and H. Ding, Phys. Rev. X **5**, 031013 (2015).
[15] S.-Y. Xu, N. Alidoust, I. Belopolski, Z. Yuan, G. Bian, T.-R. Chang, H. Zheng, V. N Strocov, D. S. Sanchez, G. Chang, C. Zhang, D. Mou, Y. Wu, L. Huang, C.-C. Lee, S.-M. Huang, B. Wang, A. Bansil, H.-T. Jeng, T. Neupert, A. Kaminski, H. Lin, S. Jia, and M. Z. Hasan, Nat. Phys. **11**, 748 (2015).

[16] L. X. Yang, Z. K. Liu, Y. Sun, H. Peng, H. F. Yang, T. Zhang, B. Zhou, Y. Zhang, Y. F. Guo, M. Rahn, D. Prabhakaran, Z. Hussain, S.-K. Mo, C. Felser, B. Yan, and Y. L. Chen, Nat. Phys. **11**, 728 (2015).

[17] B. Q. Lv, N. Xu, H. M. Weng, J. Z. Ma, P. Richard, X. C. Huang, L. X. Zhao, G. F. Chen, C. E. Matt, F. Bisti, V. N. Strocov, J. Mesot, Z. Fang, X. Dai, T. Qian, M. Shi, and H. Ding, Nat. Phys. **11**, 724 (2015).

[18] S.-Y. Xu, I. Belopolski, D. S. Sanchez, C. Zhang, G. Chang, C. Guo, G. Bian, Z. Yuan, H. Lu, T.-R. Chang, P. P. Shibayev, M. L. Prokopovych, N. Alidoust, H. Zheng, C.-C. Lee, S.-M. Huang, R. Sankar, F. Chou, C.-H. Hsu, H.-T. Jeng, A. Bansil, T. Neupert, V. N. Strocov, H. Lin, S. Jia, and M. Z. Hasan, Sci. Adv. **1**, e1501902 (2015).

[19] H. Zheng, S.-Y. Xu, G. Bian, C. Guo, G. Chang, D. S. Sanchez, I. Belopolski, C.-C. Lee, S.-M. Huang, X. Zhang, R. Sankar, N. Alidoust, T.-R. Chang, F. Wu, T. Neupert, F. Chou, H.-T. Jeng, N. Yao, A. Bansil, S. Jia, H. Lin, and M. Z. Hasan, ACS Nano **10**, 1378 (2016).

[20] H. Inoue, A. Gyenis, Z. Wang, J. Li, S. W. Oh, S. Jiang, N. Ni, B. A. Bernevig, and A. Yazdani, Science **351**, 1184 (2016).

[21] H. B. Nielsen and M. Ninomiya, Phys. Lett. B **130**, 389 (1983).

[22] S. A. Parameswaran, T. Grover, D. A. Abanin, D. A. Pesin, and A. Vishwanath, Phys. Rev. X **4**, 031035 (2014).

[23] A. C. Potter, I. Kimchi, and A. Vishwanath, Nat. Commun. **5**, 5161 (2014).

[24] Y. Baum, E. Berg, S. A. Parameswaran, and A. Stern, Phys. Rev. X **5**, 041046 (2015).

[25] A. A. Zyuzin and A. A. Burkov, Phys. Rev. B **86**, 115133 (2012).

[26] X. Huang, L. Zhao, Y. Long, P. Wang, D. Chen, Z. Yang, H. Liang, M. Xue, H. M. Weng, Z. Fang, X. Dai, and G. Chen, Phys. Rev. X **5**, 031023 (2015).

[27] C. L. Zhang, S.-Y. Xu, I. Belopolski, Z. Yuan, Z. Lin, B. Tong, G. Bian, N. Alidoust, C.-C. Lee, S.-M. Huang, T.-R. Chang, G. Chang, C.-H. Hsu, H.-T. Jeng, M. Neupane, D. S. Sanchez, H. Zheng, J. Wang, H. Lin, C. Zhang, H.-Z. Lu, S.-Q. Shen, T. Neupert, M. Z. Hasan, and S. Jia, Nat. Commun. **7**, 10735 (2016).

[28] Q. Ma, S.-Y. Xu, C.-K. Chan, C.-L. Zhang, G. Chang, Y. Lin, W. Xie, T. Palacios, H. Lin, S. Jia, P. A. Lee, P. Jarillo-Herrero, and N. Gedik, Nat. Phys. **13**, 842 (2017).

[29] C. L. Zhang, S.-Y. Xu, C. M. Wang, Z. Lin, Z. Z. Du, C. Guo, C.-C. Lee, H. Lu, Y. Feng, S.-M. Huang, G. Chang, C.-H. Hsu, H. Liu, H. Lin, L. Li, C. Zhang, J. Zhang, X.-C. Xie, T. Neupert, M. Z. Hasan, H-Z. Lu, J. Wang, and S. Jia, Nat. Phys. **13**, 979 (2017).

[30] A. A. Soluyanov, D. Gresch, Z. Wang, Q. Wu, M. Troyer, X. Dai, and B. A. Bernevig, Nature (London) **527**, 495 (2015).

[31] G. Chang, D. S. Sanchez, B. J. Wieder, S.-Y Xu, F. Schindler, I. Belopolski, S.-M. Huang, B. Singh, D. Wu, T. Neupert, T.-R. Chang, H. Lin, and M. Z. Hasan, arXiv:1611.07925.

[32] Y. Sun, S.-C. Wu, M. N. Ali, C. Felser, and B. Yan, Phys. Rev. B **92**, 161107 (2015).

[33] T.-R. Chang, S.-Y. Xu, G. Chang, C.-C. Lee, S.-M. Huang, B. Wang, G. Bian, H. Zheng, D. S. Sanchez, I. Belopolski, N. Alidoust, M. Neupane, A. Bansil, H.-T. Jeng, H. Lin, and M. Z. Hasan, Nat. Commun. **7**, 10639 (2016).

[34] B. J. Wieder, Y. Kim, A. M. Pappe, and C. L. Kane, Phys. Rev. Lett. **116**, 186402 (2016).

[35] B. Bradlyn, J. Cano, Z. Wang, M. G. Vergniory, C. Felser, R. J. Cava, and B. A. Bernevig, Science **353**, aaf5037 (2016).

[36] G. Chang, S.-Y. Xu, S.-M. Huang, D. S. Sanchez, C.-H. Hsu, G. Bian, Z.-M. Yu, I. Belopolski, N. Alidoust, H. Zheng, T.-R. Chang, H.-T. Jeng, S. A. Yang, T. Neupert, H. Lin, and M. Z. Hasan, Sci. Rep. **7**, 1688 (2017).

[37] H. Weng, C. Fang, Z. Fang, and X. Dai, Phys. Rev. B **93**, 241202 (2016).

[38] Z. Zhu, G. W. Winkler, Q. Wu, J. Li, and A. A. Soluyanov, Phys. Rev. X **6**, 031003 (2016).

[39] G. Chang, S.-Y. Xu, B. J. Wieder, D. S. Sanchez, S.-M. Huang, I. Belopolski, T.-R. Chang, S. Zhang, A. Bansil, H. Lin, and M. Z. Hasan, Phys. Rev. Lett. **119**, 206401 (2017).

[40] P. Tang, Q. Zhou, and S.-C. Zhang, Phys. Rev. Lett. **119**, 206402 (2017).

[41] T. Bzdušek, Q. Wu, A. Rüegg, M. Sigrist, and A. A. Soluyanov, Nature (London) **538**, 75 (2016).

[42] G. Chang, S.-Y. Xu, X. Zhou, S.-M. Huang, B. Singh, B. Wang, I. Belopolski, J. Yin, S. Zhang, A. Bansil, H. Lin, and M. Z. Hasan, Phys. Rev. Lett. **119**, 156401 (2017).

[43] F. de Juan, A. G. Grushin, T. Morimoto, and J. E. Moore, Nat. Commun. **8**, 15995 (2017).

[44] S.-Y. Xu, N. Alidoust, G. Chang, H. Lu, B. Singh, I. Belopolski, D. S. Sanchez, X. Zhang, G. Bian, M.-A. Husanu, Y. Bian, S.-M. Huang, C.-H. Hsu, T.-R. Chang, H.-T. Jeng, A. Bansil, T. Neupert, V. N. Strocov, H. Lin, S. Jia, and M. Z. Hasan, Sci. Adv. **3**, e1603266 (2017).

[45] L. Huang, T. M. McCormick, M. Ochi, Z. Zhao, M.-T. Suzuki, R. Arita, Y. Wu, D. Mou, H. Cao, J. Yan, N. Trivedi, and A. Kaminski, Nature Mater. **15**, 1155 (2016).

[46] K. Deng, G. Wan, P. Deng, K. Zhang, S. Ding, E. Wang, M. Yan, H. Huang, H. Zhang, Z. Xu, J. Denlinger, A. Fedorov, H. Yang, W. Duan, H. Yao, Y. Wu, S. Fan, H. Zhang, X. Chen, and S. Zhou, Nat. Phys. **12**, 1105 (2016).

[47] I. Belopolski, D. S. Sanchez, Y. Ishida, X. Pan, P. Yu, S.-Y. Xu, G. Chang, T.-R. Chang, H. Zheng, N. Alidoust, G. Bian, M. Neupane, S.-M. Huang, C.-C. Lee, Y. Song, H. Bu, G. Wang, S. Li, G. Eda, H.-T. Jeng, T. Kondo, H. Lin, Z. Liu, F. Song, S. Shin, and M. Z. Hasan, Nat. Commun. **7**, 13643 (2016).

[48] A. Tamai, Q. S. Wu, I. Cucchi, F. Y. Bruno, S. Riccò, T. K. Kim, M. Hoesch, C. Barreteau, E. Giannini, C. Besnard, and A. A. Soluyanov, and F. Baumberger, Phys. Rev. X **6**, 031021 (2016).

[49] H. Zheng, G. Bian, G. Chang, H. Lu, S.-Y. Xu, G. Wang, T.-R. Chang, S. Zhang, I. Belopolski, N. Alidoust, D. S. Sanchez, F. Song, H.-T. Jeng, N. Yao, A. Bansil, S. Jia, H. Lin, and M. Z. Hasan, Phys. Rev. Lett. **117**, 266804 (2017).

[50] G. Bian, T.-R. Chang, R. Sankar, S.-Y. Xu, H. Zheng, T. Neupert, C.-K. Chiu, S.-M. Huang, G. Chang, I. Belopolski, D. S. Sanchez, M. Neupane, N. Alidoust, C. Liu, B. Wang, C.-C. Lee, H.-T. Jeng, C. Zhang, Z. Yuan, S. Jia, A. Bansil, F. Chou, H. Lin, and M. Z. Hasan, Nat. Commun. **7**, 10556 (2016).

[51] B. Q. Lv, Z.-L. Feng, Q.-N. Xu, X. Gao, J.-Z. Ma, L.-Y. Kong, P. Richard, Y.-B. Huang, V. N. Strocov, C. Fang, H.-M. Weng, Y.-G. Shi, T. Qian, and H. Ding, Nature (London) **546**, 627 (2017).

[52] G. Xu, H. Weng, Z. Wang, X. Dai, and Z. Fang, Phys. Rev. Lett. **107**, 186806 (2011).

[53] M. C. Shapiro, S. C. Riggs, M. B. Stone, C. R. de la Cruz, S. Chi, A. A. Podlesnyak, and I. R. Fisher, Phys. Rev. B **85**, 214434 (2012).

[54] K.-Y. Yang, Y.-M. Lu, and Y. Ran, Phys. Rev. B **84**, 075129 (2011).
[55] S. Borisenko, D. Evtushinsky, Q. Gibson, A. Yaresko, T. Kim, M. N. Ali, B. Buechner, M. Hoesch, and R. J. Cava, arXiv:1507.04847.
[56] A. A. Burkov, Phys. Rev. Lett. **113**, 187202 (2014).
[57] M. Kargarian, M. Randeria, and N. Trivedi, Sci. Rep. **5**, 12683 (2015).
[58] A. M. Guloy and J. D. Corbett, Inorg. Chem. **30**, 4789 (1991).
[59] S. K. Dhar and S. M. Corbett, J. Magn. Magn. Mater. **152**, 22 (1996).
[60] E. I. Gladyshevskii, N. Z Nakonechna, K Cenzual, R. E. Gladyshevskii, and J.-L. Jorda, J. Alloys Compd. **296**, 265 (2000).
[61] S. K. Dhar and S. M. Pattalwar, J. Magn. Magn. Mater. **104**, 1303 (1992).
[62] S. Bobev, P. H. Tobash, V. Fritsch, J. D. Thompson, M. F. Hundley, J. L. Sarrao, and Z. Fiskc, J. Solid State Chem. **178**, 2091 (2005).
[63] H. Flandorfer, D. Kaczorowski, J. Gröbner, P. Rogl, R. Wouters, C. Godart, and A. Kostikas, J. Solid State Chem. **137**, 191 (1998).
[64] J. Wang, B. Lian, and S.-C. Zhang, arXiv:1607.00116.
[65] S. Murakami, New J. Phys. **9**, 356 (2007).
[66] See Supplemental Material at http://link.aps.org/supplemental/10.1103/PhysRevB.97.041104 for the details of our first-principles electronic calculation methods, energy dispersion, and momentum distribution of the Weyl fermions in the *R*AlGe family and effective Hamiltonian for the $W3$ nodes. Which include Refs. [69–71].
[67] C.-Z. Chen, J. Song, H. Jiang, Q.-F. Sun, Z. Wang, and X. C. Xie, Phys. Rev. Lett. **115**, 246603 (2015).
[68] H. Shapourian and T. L. Hughes, Phys. Rev. B **93**, 075108 (2016).
[69] G. Kresse and D. Joubert, Phys. Rev. B **59**, 1758 (1999).
[70] G. Kresse and J. Furthmller, Comput. Mater. Sci. **6**, 15 (1996).
[71] J. P. Perdew, K. Burke, and M. Ernzerhof, Phys. Rev. Lett. **77**, 3865 (1996).